Available online at www.sciencedirect.com
ScienceDirect
Journal of the European Ceramic Society 29 (2009) 943–948
www.elsevier.com/locate/jeurceramsoc

Characterization of particles packing in alumina green tape

N. Chantaramee *, S. Tanaka, Z. Kato, N. Uchida, K. Uematsu

Department of Materials Science and Technology, Nagaoka University of Technology, 1603-1, Kamitomioka, Nagaoka, Niigata 940-2188 Japan

Available online 28 August 2008

Abstract

Aqueous alumina slurry was prepared with a commercial powder of elongated particles, which has the aspect ratio ranging from 1 to 3.5 with the mean of 1.6, to examine the effect of forming conditions on the particle alignment in green tapes. The slurry appeared pseudoplastic with a yield stress, but showed no thixotropic behavior. Its flow curve fitted very well to the Herschel–Bulkley model approximation, which suggested shear-thinning constant of 0.54. Polarized microscopy with the liquid immersion technique was applied to examine the particle orientation through the direction along the tape thickness. In the absence of coquette flow, randomly oriented particles were noted in the tape. At the top surface, particles were aligned with their long-axes (*a*-axis) along the casting direction. The variation in the degree of orientation was 6.8 ± 1.2. In the area near the Mylar carrier, *a*-axis of particle made an angle to the carrier surface with the degree of orientation about 5.8 ± 1.0. As the combination of pressure flow and coquette flow, tape cast with casting velocity of 2.5 and 91.5 cm/min, which respectively resulted in shear rate of 1.38 and 50.8 s^{-1}, were observed. The orientation was significant near the top surface and was higher than that above the carrier surface. The *a*-axis of particles above the carrier surface was inclined to the surface at low shear rate (1.38 s^{-1}), but was nearly parallel at high shear rate (50.8 s^{-1}). Nevertheless, the orientation varies with the location in the tape prepared at the shear rate of 50.8 s^{-1}.

Keywords: Alumina; Tape casting; Particle orientation; Anisotropic packing structure

1. Introduction

Delamination, warpage and cracks are often noted in the tape casting products. Mismatch in sintering kinetic, sintering stresses, density variation between tape layers are well documented to play an important role in the curvature development.[1,2] Non-uniform shrinkage and resultant deformation in individual tape itself must also be important for the formation of these defects. Recent studies showed anisotropic packing structure of particles and its influence on the anisotropic shrinkage.[3–5] The powder characteristic, especially the particle shape also played an important role.[6] Thus, understanding the tape texture during forming is very important to diminish undesirable deformation.

In this study, alumina powder is chosen as a starting powder for aqueous slurry. The powder is often employed in tape casting process for alumina-based layer composites such as Al_2O_3/ZrO_2, Al_2O_3/Y-TZP, Al_2O_3/TiC, $Al_2O_3/MoSi_2$ and so on.[7–12] The powder has a slightly anisotropic shape and may orient in the shear field with only a few degree. Since, *c*-plane of alumina shows only very weak peak in the X-ray diffraction analysis, which makes difficulty on accurate evaluation of particle orientation. A special characterization method based on optical microscopy had to be employed to evaluate for the particle orientation. The main objective of this study is to evaluate the particles packing structure in aqueous alumina green sheet. The packing structure of the cross-section of the casting direction will be mainly examined because it represents for the slurry flow below the doctor blade.

2. Experimental procedure

2.1. Slurry and sample preparation

Alumina green tapes were prepared from α-alumina powder (AL160SG1, Showa Denko, Japan). Nominal average particle size and the specific surface area of the powder were 0.6 μm and 6 m^2/g, respectively. The particle shape including length and width was observed with SEM (JSM-T100, JEOL, Japan). Aqueous alumina slurry with the solid loading of 43 vol% was prepared with ammonium polyacrylate (D305, Chukyoyushi, Japan) as the dispersant (0.6 wt.%), polyvinyl alcohol (LA-05GP, Shin-Etsu Chemical, Japan) as the binder

* Corresponding author. Tel.: +81 258 47 9317; fax: +81 258 47 9337.
E-mail address: chantaramee_napat@mst.nagaokaut.ac.jp
(N. Chantaramee).

0955-2219/$ – see front matter © 2008 Elsevier Ltd. All rights reserved.
doi:10.1016/j.jeurceramsoc.2008.07.032

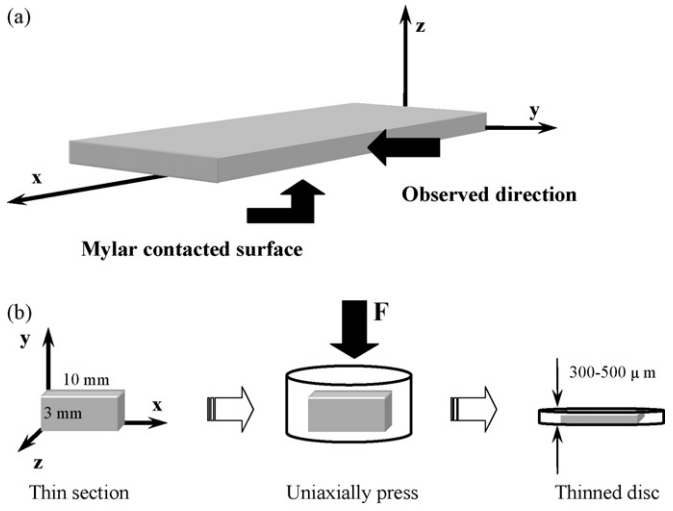

Fig. 1. Notation of (a) tape axes in three-dimension and (b) outline of sample preparation.

(11 wt.%) and glycerol (Kanto Chemical, Japan) as the plasticizer (1 wt.%).

The slurry viscosity was measured by a viscometer (VT550, Haake, Germany) with a coaxial cylinder sensor system (ISO3219/DIN53019). The sample was left to equilibrium $25 \pm 0.5\,^{\circ}C$ before measurement. The profile of shear rate in the measurement was as follows; the shear rate was increased from 0 to $500\,s^{-1}$ in a time period of 5 min, and then reversed to $0\,s^{-1}$ in 5 min, followed by a rest for 1 min, and then the next cycle was performed in the same manner. The second cycle of the measurement was used to analyze the flow behavior of the slurry. The thixotropic behavior was investigated in the controlled shear rate of 1 and $55\,s^{-1}$ at constant temperature of $25 \pm 0.5\,^{\circ}C$.

Tape casting was performed with a laboratory tape cast bench with a stationary double blade system (DP-150, Sayama Riken, Japan). The tape axes were referred to *x*-axis for the casting direction, *y*-axis for the cross-casting direction, and *z*-axis for the tape thickness direction, illustrated in Fig. 1a. The blade geometry is as described in Fig. 2. Slurries were cast on a silicone coated Mylar sheet moving at a constant velocity of 2.5 and 91.5 cm/min. The green tapes, with *x*–*y* dimensions of 90 cm × 15 cm, were allowed to dry at an ambient temperature

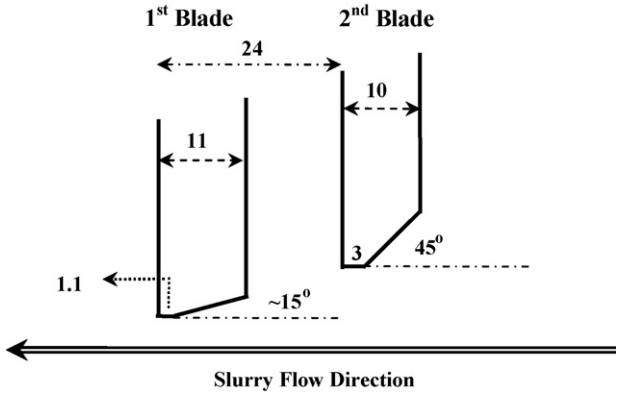

Fig. 2. Blade geometry (dimension unit in mm).

for 24 h. The tapes thickness was measured with a micrometer. To examine the structure in *x*–*z* plane of the cast tape, the green tapes were cut into sections with *x*–*y* dimension of 10 mm × 3 mm. Each section was placed into alumina granules (TM-DS6, Taimai Chemical Co., Ltd., Japan), which show optically isotropic characteristic when observe under polarized light microscope with the liquid immersion technique, to facilitate handling during grinding. The disc-like specimen (Fig. 1b) was obtained after uniaxially pressed at ~3 MPa, followed by heated up to 1000 °C with the heating rate of 10 °C/min in order to remove organic components and allow inter-particles contact. Prior to measurement of particle orientation by optical microscopy technique, the discs were thinned with an abrasive paper to the thickness of 300–500 μm.

2.2. Particle orientation measurement

The particle orientation was observed by polarized light microscope with the liquid immersion technique.[13] The thinned specimen was immersed into diiodomethane (Refractive index 1.77) for 15 min to make a nearly transparent sample. The alignment of alumina particles, in the cross-section parallel to the casting direction (*x*–*z* plane), was observed under a crossed polarized light microscope (OPTIPHOT2-POL, Nikon, Japan) with a white light in the transmission mode.

The concept of measurement based on the ray-velocity surface, sphere whose radius is proportional to the velocity of light. Diagram illustrated the concept of ray-velocity surface for positive uniaxial crystal is shown in Fig. 3a. The *c*-axis of alumina hexagonal crystal is identical to the optical axis. The ray-velocity surface for ordinary ray (o-ray) is a sphere indicates for the equal velocity in all direction, while the ray-velocity surface for extraordinary ray (e-ray) is an ellipsoid which represents for the varying of velocity in different directions. In the opti-

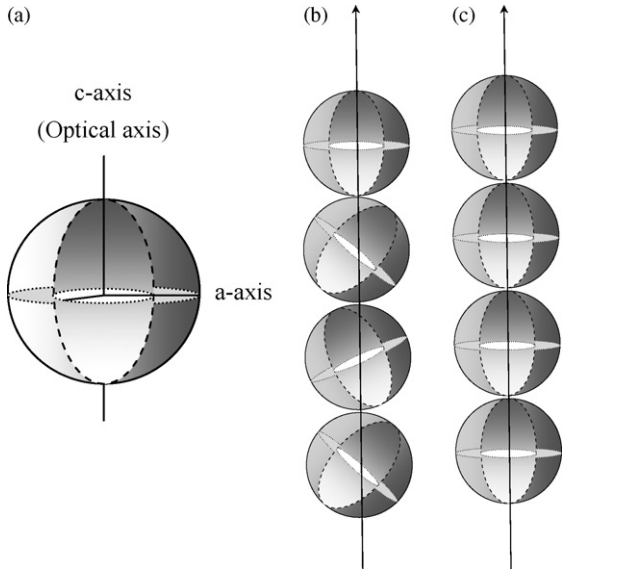

Fig. 3. The ray-velocity surface (a) 3D Ray-velocity surface of positive uniaxial crystal, (b) light direction makes some angle to optical axis and (c) light propagates in optical axis direction.

cal axis direction, the velocities of the o-ray and the e-ray are equal. If polarized light propagates along an off-axis direction in an uniaxial crystal, the optical path difference or retardation is introduced from velocity difference between the o-ray and the e-ray.[14] Fig. 3b shows light passing through the crystal at a certain angle to the optical axis, and finally creates retardation. Fig. 3c shows light traveling in the optical axis direction. Both rays travel at the same velocity, thus there is no retardation.

A Berek compensator was used to measure the retardation angle. The retardation (R) of the sample can be calculated from relationship between the retardation and birefringence (Δn) of the sample, shown in Eq. (1),[15]

$$R = d\rho\Delta n \tag{1}$$

where, d is the sample thickness and ρ is the relative density measured by the Hg-porosimeter (Model 9310, Shimadzu, Japan). Orientation degree (f), defined as the ratio between the birefringence of sample and the birefringence of alumina single crystal (0.0075), was calculated from Eq. (2)

$$f(\%) = \frac{\Delta n_{\text{sample}}}{\Delta n_{\text{single crystal}}} \times 100. \tag{2}$$

3. Results and discussion

3.1. Alumina particle characteristic

Fig. 4 shows the aspect ratio distribution. Alumina powder composes of agglomerated particles and shows elongated shape. Length and width of 210 particles were measured, resulted in aspect ratio from 1 to 3.5 with a mean of 1.6.

3.2. Slurry characteristic

Fig. 5 shows apparent viscosity of slurry. It decreases as the shear rate increases, exhibiting shear-thinning behavior with the yield stress. Herschel–Bulkley model as in Eq. (3) provides the best fit for the measured flow data, where σ, k and $\dot{\gamma}$ are shear stress, Herschel–Bulkley viscosity and shear rate, respectively.

$$\sigma = \sigma_y + k\dot{\gamma}^n \tag{3}$$

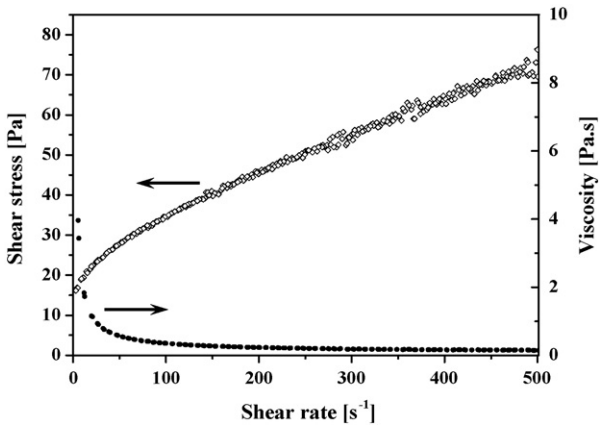

Fig. 5. Flow characteristic of model slurry.

The yield stress, σ_y, predicted from Herschel–Bulkley model is approximately 12.7 Pa s. The shear thinning constant, n, is 0.54.

Fig. 6 shows apparent viscosity as a function of time according to the sequence of shear rate step. Apparent viscosity change immediately after the shear rate is switched either from 1 to 55 s^{-1} or from 55 to 1 s^{-1}. It suggests for the time-independent behavior.

3.3. Particle orientation observed from green tape

Fig. 7 shows cross-polarized light images of the pressure flow slurry. The specimen was prepared as follow. At First, carrier velocity was adjusted to zero. The caster equipped without the 1st blade, then slurry was allowed to flow beneath the 2nd blade while the slurry height in the reservoir maintained constant. The flow of slurry was governed only by the hydrostatic pressure.

The initial part of slurry that passed under the blade is at the left tip in the figure. In Fig. 7a, the blue color appears in the area near the carrier surface. The upper portion above the blue shows pink color and remains the same color even after the rotation of the microscope stage for 45° as is shown in Fig. 7b. The difference of color indicates the difference in direction of optical

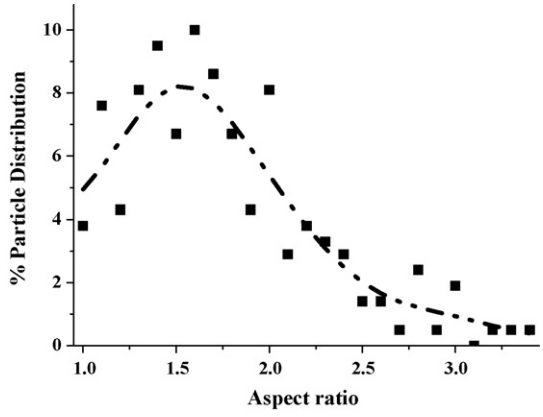

Fig. 4. Aspect ratio distribution of alumina particle.

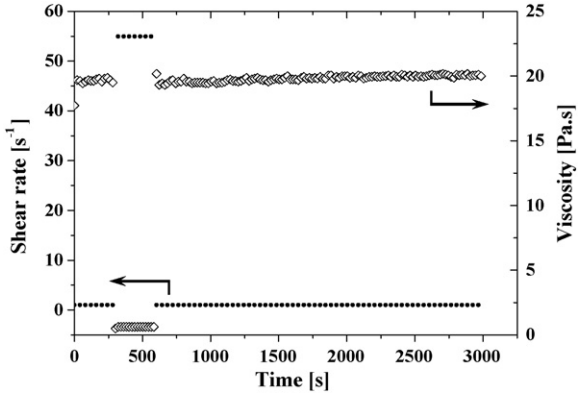

Fig. 6. Apparent viscosity as a function of time.

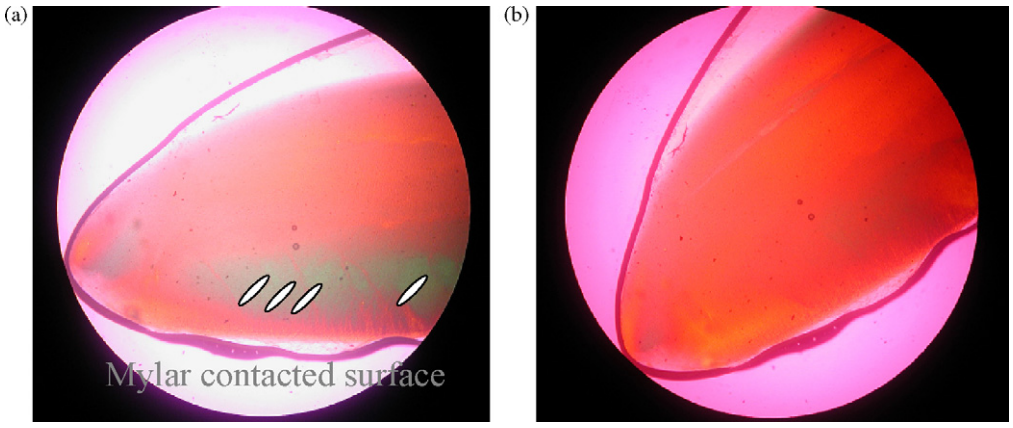

Fig. 7. Cross-polarized light images of pressure flow slurry (a) at microscope stage = 0° (b) at microscope stage = +45°.

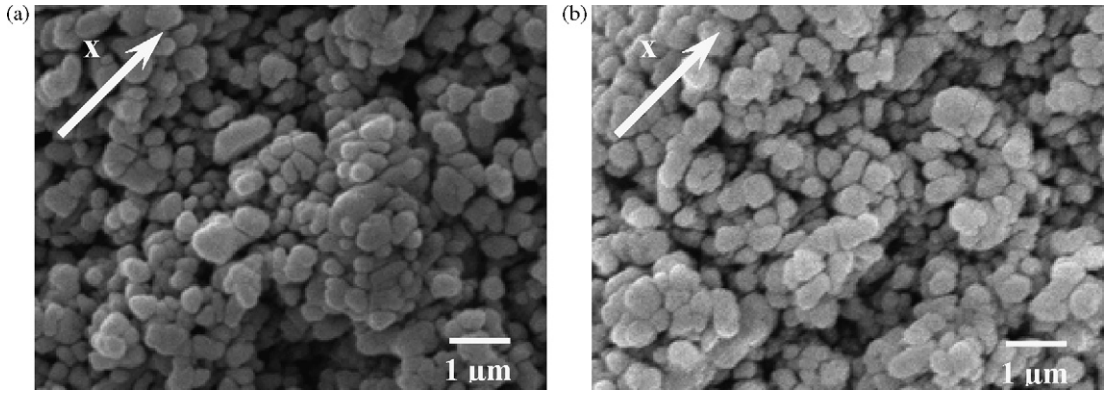

Fig. 8. SEM micrographs of alumina green tape (x–z plane) calcined at 1000 °C (a) $\dot{\gamma} = 1.38\,s^{-1}$ and (b) $\dot{\gamma} = 50.8\,s^{-1}$.

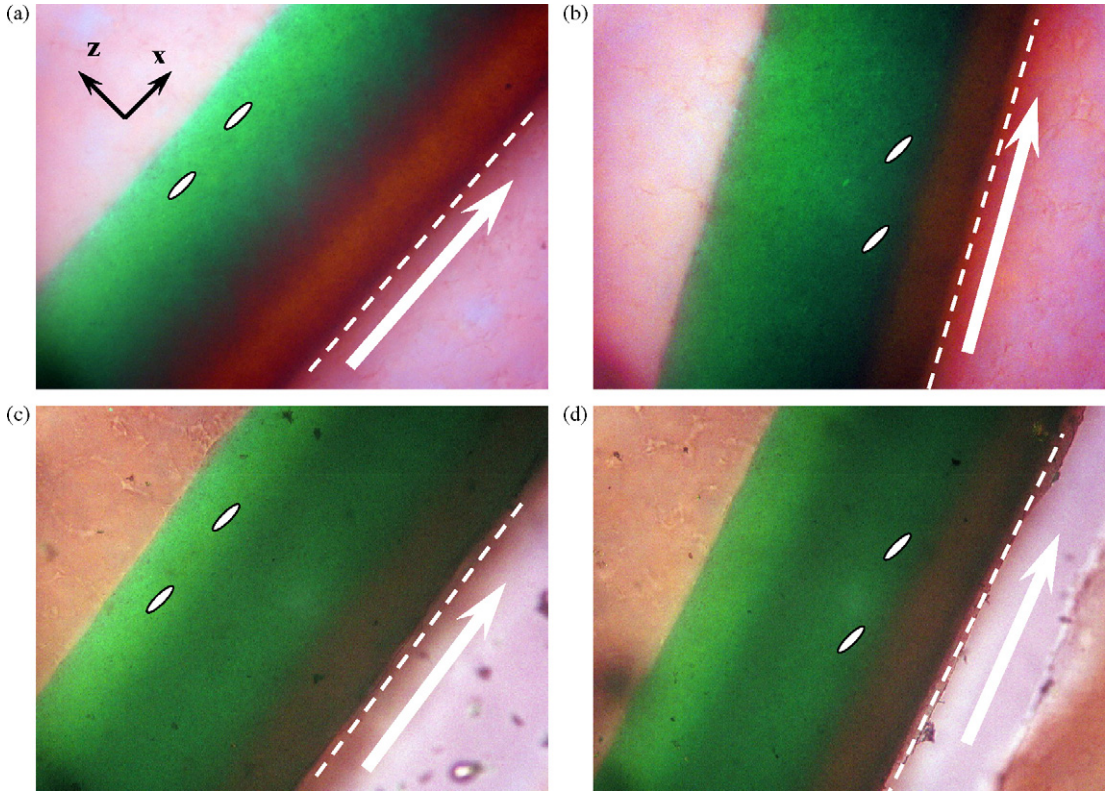

Fig. 9. Cross-polarized light images indicate maximum interference of light of (a) top surface $\dot{\gamma} = 1.38\,s^{-1}$, (b) Mylar contacted surface $\dot{\gamma} = 1.38\,s^{-1}$, (c) top surface $\dot{\gamma} = 50.8\,s^{-1}$ and (d) Mylar contacted surface $\dot{\gamma} = 50.8\,s^{-1}$.

axis and obviously suggests for randomly oriented particles in the middle area. The particle orientation degrees were 5.8 ± 1.0 and 6.8 ± 1.2 for the area near the carrier surface and the top surface, respectively. Clearly, the long-axes (*a*- or *b*-axes) of particles embedded near the carrier surface inclined to the surface. Whereas, at the top surface, their alignment are nearly parallel to the flow direction. The white ellipses in Fig. 7a represents for the alignment pattern of particles.

In the combination of pressure flow and coquette flow, slurries were cast at a velocity of 2.5 and 91.5 cm/min using a stationary double blades unit. The casting velocities resulted in the processing shear rate of 1.38 and 50.8 s^{-1}, respectively.

Fig. 8 shows the microstructure of alumina green tape sheared along the casting direction, refers as *x*-direction. Some elongated particles are aligned in the sheared direction, but there was no significant difference in the overall particles alignment if observed directly from SEM micrograph for both shear rates of 1.38 and 50.8 s^{-1}. However, particles orientation can evaluated from SEM micrograph as reported in edge orientation polarlogram technique.[6]

Fig. 9 shows the structure images under crossed polarized light. Micrographs were taken along the *y*-direction (*x*–*z* plane). The white arrow indicates the casting direction and the dashed line signifies the carrier contacted surface. Fig. 9a and c indicates maximum interference of light at top surface. Three-fourths of the tape appears in blue color but the remains of tape show pink color. The particles packing determined from the interference of light are sketched as white ellipses; the longest-axes aligned in the casting direction. In the pink area, the long-axes align with difference direction. Fig. 9b and d shows maximum interference of light at the area above the carrier surface. The long-axes of particles, which embedded above the carrier surface, are deviated from the casting direction and inclined to the surface. However, the long-axes alignments are nearly turn in the casting direction when process by shear rate of 50.8 s^{-1}. Possible explanations for the alignment above the carrier surface include the blade geometry that creates vortex during flow, short distance of exit channel and the non-uniform shear rate distribution under blade.

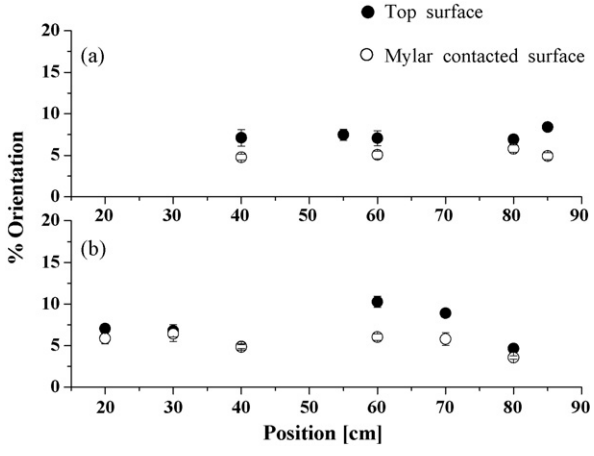

Fig. 10. Orientation degree along green tape by (a) $\dot{\gamma} = 1.38\ s^{-1}$ and (b) $\dot{\gamma} = 50.8\ s^{-1}$.

Fig. 10 shows orientation degree at various positions along the green sheet. Remarkable orientation was observed for all regions. The top surface shows slightly stronger orientation than the region above the carrier surface. More uniform orientation is noted in the sheet prepared at the shear rate of 1.38 than 50.8 s^{-1}.

4. Summary

Particles packing in alumina green tape and orientation degrees were evaluated via optical technique under polarized microscope. The initial part of pressure flow slurry showed random aligned particles except area above the carrier surface and blade-contacted surface. However, the long-axes of particles somehow aligned in difference direction, e.g. co-linear to the flow direction at top surface but inclined with acute angle to carrier surface. By the combination of pressure flow and couette flow, as expected for the top surface, the long-axes aligned in the casting direction. However, at above the carrier surface, the long-axes of particles showed some degree of deviation from the casting direction. The cast tape using shear rate of 50.8 s^{-1} showed less degree of deviation than that cast by shear rate of 1.38 s^{-1}. In addition, stronger orientation degrees were observed at the upper surface rather than at the lower surface.

References

1. Lu, G. Q., Sutterlin, R. C. and Gupta, T. K., Effect of mismatched sintering kinetics on camber in a low-temperature cofired ceramic package. *J. Am. Ceram. Soc.*, 1993, **76**(8), 1907–1914.
2. Ravi, D. and Green, D. J., Sintering stresses and distortion produced by density differences in bi-layer structure. *J. Eur. Ceram. Soc.*, 2006, **26**(1/2), 17–25.
3. Uematsu, K., Ishaka, S., Shinohara, N. and Okumiya, M., Grain-oriented microstructure of alumina ceramics made through the injection molding process. *J. Am. Ceram. Soc.*, 1997, **80**(5), 1313–1315.
4. Sung, J. S., Koo, K. D. and Park, J. H., Lamination and sintering shrinkage behavior in multilayered ceramics. *J. Am. Ceram. Soc.*, 1999, **82**(3), 537–544.
5. Shui, A., Uchida, N. and Uematsu, K., Origin of shrinkage anisotropy during sintering for uniaxially pressed alumina compacts. *Powder Technol.*, 2002, **127**, 9–18.
6. Raj, P. M. and Cannon, W. R., Anisotropic shrinkage in tape-cast alumina: role of processing parameters and particle shape. *J. Am. Ceram. Soc.*, 1999, **82**(10), 2619–2625.
7. Mistler, R. E. and Twiname, E. R., *Tape casting theory and practice*. Am. Ceram. Soc., Westerville, OH, 2000.
8. Pluncknett, K. P., Caceres, C. H. and Wilkinson, D. S., Tape casting of fine alumina/zirconia powders for composite fabrication. *J. Am. Ceram. Soc.*, 1994, **77**(8), 2137–2144.
9. Pluncknett, K. P., Caceres, C. H., Hughes, C. and Wilkinson, D. S., Processing of tape-cast laminates prepared from fine alumina/zirconia powders. *J. Am. Ceram. Soc.*, 1994, **77**(8), 2145–2153.
10. Gurauskis, J., Sanchez-Herencia, A. J. and Baudin, C., Al_2O_3/Y-TZP and Y-TZP materials fabricated by stacking layers obtained by aqueous tape casting. *J. Eur. Ceram. Soc.*, 2006, **26**(8), 1489–1496.
11. Yu-Ping, Z., Dong-Liang, J. and Watanabe, T., Fabrication and properties of tape-cast laminated and functionally gradient alumina–titanium carbide materials. *J. Am. Ceram. Soc.*, 2000, **83**(12), 2999–3003.
12. Watanabe, T., Zhang, G. J., Yue, X. M., Zeng, Y. P., Shobu, K. and Bahlawance, N., Multilayer composites in Al_2O_3/$MoSi_2$ system. *Mater. Chem. Phys.*, 2000, **67**, 256–326.

13. Uematsu, K., Zhang, Y. and Ito, N., Novel characterization method for the processing of ceramics by polarized microscope with liquid immersion technique. *Ceram. Trans.*, 1995, **51**, 273–280.
14. Robinson, P. C. and Savile, B., *Qualitative polarized-light microscopy*. Oxford University Press and Royal Microscopical Soceity, 1992, pp. 10–14.
15. Tanaka, S., Makiya, A., Watanabe, S., Kato, Z., Uchida, N. and Uematsu, K., Particle orientation distribution in alumina compact body prepared by the slip casting method. *J. Ceram. Soc. Jpn.*, 2004, **112**(5), 276–279.